한국해양공학회지 제19권 제3호, pp 47~53, 2005 (ISSN 1225-0767)

Salt and Sand Transport from Aral Sea Basin

KWI-JOO LEE*, IGOR-SHUGAN*, NA-RA PARK*
A. BEGMATOV**, N.T. MAMATOVA**,
AND CHUNG-HWAN LEE***
*Dept. of Naval Architecture and Ocean Engineering, Chosun University, Gwangju, Korea
**Tashkent State University, Vuzgorodok, Tashkent Geoje, Korea Uzbekistan
***Samsung Heavy Industries

KEY WORDS: Dust Transportation 먼지 수송, Turbulent Diffusion 난류의 확산, 아랄해 Catastrophe 아랄해 대참사.

ABSTRACT: *Model for dust and salt transportation from the dried bottom of the Aral Sea is suggested. Theoretical analysis is based on the turbulent diffusion equation for the averaged function of passive impurity concentration. One-layer model of the atmospheric boundary layer is assumed. Impurity precipitation rates are calculated as the functions of the particle size and the distance source of particles. Analytical solutions for the point and two-dimensional sources of impurities are found. Model calculations for salt and sand transport from the Aral Sea basin are made on the basis of 2D source model with a constant intensity.*

1.INTRODUCTION

The fatal consequence of the Aral Sea depression (from the maximum absolute value of 53.40m in 1960 to 36.60m in 1994) is an increase in the seawater salinity and expansion of drained areas and saline lands. In the 1960s the average salinity was 10g · kg-1, as investigated by Tolkachyova (2000), while in 1995 it was 40g · kg-1, that is, the Aral Sea has transformed from saltish to salty. This has disturbed the Sea's ecosystem: the population of microorganisms has shrunk, the biomass has decreased several times, the fishery has abruptly reduced and, finally, the salt emission intensity from the sea water area has increased (from 277g · kg-2 in 1957 to about 150g · kg-2 in 1990). A similar increase in the salt and saliferous dust removal, observed in the drained area of the Aral Sea and in saline lands, is promoted by a decrease in the humidity content in the lower atmosphere and an increase in frequency of dusty storms. A significant depression of subsoil waters in the drained area and beyond it, which results in the drying of the upper soil layer, is observed.

제1저자 이귀주 연락처: 광주광역시 동구 서석동 375번지
062-230-7075 kjalee@chosun.ac.kr

As a result, a huge mass of salt is removed annually from these territories of the sea water area, the drained area, and saline lands. According to some calculations, in 1990 along the total mass of removed salts was 120 million tons. This mass is carried by wind over long distances.

From 70 to 100kg/hectare of salts per year are precipitated in the Bukhara region (more than 500km from sea). Therefore, it becomes important to forecast the transport and precipitation of salt and sand removed from the Aral Sea basin. Many studies are devoted to the numerical simulation of the atmospheric transport and precipitation of salts as applied to the estimation of the ecological state of the Aral Sea basin (see, for example, Tolkachyova, 2000; Berlyand, 1975 and 1985). The propagation of industrial pollutions was calculated within a diffusion model by Berlyand (1975) and Marchuk (1982). Contamination transport was estimated under the assumption of the Gaussian distribution of impurities by Berlyand (1985).

In this study, we develop a diffusion model of impurity transport for ground-based sources. Point and two-dimensional (2D) sources for one-layer model of the atmospheric boundary layer were considered. Model calculations for the Aral basin were carried out and the characteristic dependences of solid impurity transport were analyzed.

2. MODEL OF TURBULENT DIFFUSION AND PROPAGATION OF IMPURITIES IN THE ATMOSPHERE

Various problems associated with impurity propagation in the atmosphere were studied by Kolmogorov (1991), Obukhov (1962), Monin and Yaglom (1979), Richardson (1922) and others. Their basic concepts and the solution of the problems of impurity propagation are given in the paper by Berlyand (1975). The models for calculating impurity transport in the atmosphere are conventionally constructed on the basis of the turbulent diffusion equation for the averaged function of impurity concentration (Berlyand, 1975),

$$\frac{\partial c}{\partial t}+u\frac{\partial c}{\partial x}+v\frac{\partial c}{\partial y}+w\frac{\partial c}{\partial z}=\frac{\partial c}{\partial x}\left(k_x\frac{\partial c}{\partial x}\right)+\frac{\partial c}{\partial y}\left(k_y\frac{\partial c}{\partial y}\right)+\frac{\partial c}{\partial z}\left(k_z\frac{\partial c}{\partial z}\right)-\alpha c=0 \qquad (1)$$

where $c(x, y, z, t)$ is the average concentration; x and y are the horizontal axes, z is the vertical axis; t is the time; k_x, k_y and k_z are the components of the turbulent exchange coefficient; u, v and w are the components of the average motion velocity; and α is the coefficient defining the concentration change due to impurity transformation. The transport velocities and the turbulent exchange coefficients in Eq.(1) are assumed to be defined functions of the coordinates and time.

In practical calculations, the following simplifications are generally applicable.

(i) The wind velocity field is one-dimensional in the horizontal plane; if the x axis is directed downwind, we can accept $v=0$.

(ii) Advective impurity transport with the wind significantly exceeds the diffusion one; therefore, the latter can be neglected, that is, we can set $k_x=0$ in Eq.(1). We note that this approximation can be invalid if the terrain has significant variations where the rates of change of functions over all the space variables become comparable.

(iii) Of prime interest is the calculation of steady modes of impurity transport at times exceeding (in the order of magnitude) the time $t\sim x/u$ of transient processes; therefore, it is set as $\partial c/\partial t=0$ by Berlyand (1975), Lysak and Ryaboshenko (1987) and Marchuk (1982).

Thus, neglecting also phase transformation of impurities, Eq.(1), takes on the form

$$u\frac{\partial c}{\partial x}+w\frac{\partial c}{\partial z}=\frac{\partial}{\partial y}\left(k_y\frac{\partial c}{\partial y}\right)+\frac{\partial}{\partial z}\left(k_z\frac{\partial c}{\partial z}\right) \qquad (2)$$

The vertical velocity component also takes into account both vertical flows and the precipitation rate of solid particles. With no vertical flows, it is set as

$$w=-w_0 \qquad (3)$$

where w_0 is the precipitation rate of solid particles. For sufficiently small particles, the light impurity approximation by Berlyand (1975) is also used, $w_0=0$.

2.1 Diffusion coefficients in Eq.(2)

As is known, atmospheric processes are stratified. For example, when studying impurity propagation in the atmosphere, bottom and boundary atmospheric layers of thicknesses $h\approx$50-100m and $h\approx$1km, respectively, are distinguished. In the surface atmospheric layer, the altitudes of the vertical heat flow and momenta mostly remain unchanged. However, wind velocity, temperature, and characteristic turbulence scales reveal significant altitude variations.

The turbulent exchange coefficient k_z was determined in the studies by Batchelor (1953), McComb (1992) and Berlyand (1985). The main conclusion of these studies is the approximate formula

$$k=k_1\times\frac{z}{z_1} \qquad (4)$$

valid in the surface atmospheric layer $(0\le z\le h)$ where k_1 is constant, z_1 is the unit altitude from the ground, often set as 1m.

If we assume that the friction stress and the heat flow in the surface layer are unchanged, then, according to the law of conservation of momentum, the wind velocity and temperature logarithmically vary with altitude.

The Yudin and Shvets model is considered to be acceptable in most cases of calculating the near-ground concentrations (Berlyand, 1975),

$$u=u_1\frac{\log(z/z_0)}{\log(z_1/z_0)},\quad k_2=\begin{cases}\nu+k_1\dfrac{z}{z_1}, & z\le h,\\ \nu+k_1\dfrac{h}{z_1}, & z>h.\end{cases} \qquad (5)$$

where $\nu=k_{z|z=0}$ is the molecular diffusion coefficient generally set to zero, and z_0 is the surface roughness.

It follows from Eq.(5) that vortex sizes at $z>h$ weakly vary with altitude; hence it may be accepted that atmospheric turbulence is isotropic,

$$k_x \cong k_y \cong k_z \tag{6}$$

At $z < h$, the variation rate of the horizontal components of turbulent exchange with altitude can be estimated by the Berlyand hypothesis (Berlyand, 1975), which significantly simplifies analytical studies and has the sufficiently justified functional form

$$k_x = k_y = k_0 u \tag{7}$$

where k_0 is the constant determined from boundary conditions Eq.(5) at the outer boundary of the surface atmospheric layer.

The precipitation rate w_0 of solid particles at $Re = w_0 d/v < 1$ is determined using the Stokes formula (Begmatov et al., 2002)

$$w_0 = \frac{2}{9}\frac{\rho}{\rho_a}\frac{g}{v}r^2 \tag{8}$$

where ρ and ρ_a are the dust and air particle densities, respectively, r is the particle radius, g is the gravity acceleration, and v is the kinematic viscosity of air. At large Reynolds numbers, the precipitation rate of solid particles was determined by the corrections of the Stokes formula by Loitsyansky (1970).

2.2 Simulation of salt and sand removal from the Aral Sea basin on the basis of turbulent diffusion Eq.(2)

According to numerous studies, in the Aral sea basin salt and sand are removed from sea water, drained territories, and saline lands. According to the calculations of Tolkachyova (2000), the salt mass removed in 1990 is distributed as is shown in Table 1. The total removal of salts from the Aral Sea basin is 1,210,596,883 tons.

Table 1 Salt removal from Aral Sea basin in 1990

	Area, km^2	Salt mass, ton · km^{-2}	Total removal, ton · km^{-2}
Sea water area	3500	1274.25	598750
Drained area	52389	1764.78	57059359
Saline lands	4292.0	4645.8	1993877

These quantitative indicators of course have a certain error. First, a more detailed distribution of salt removal over each region (the sea water area, drained area, and saline lands) is too difficult to calculate; second, the error is unlikely to be smaller. Finally, even detailed time distribution of salt removal over the Aral Sea basin will hardly raise the efficiency of a year-long salt removal forecast because of large errors in the forecast of atmospheric processes for such long time intervals.

Therefore, in our opinion, it would be reasonable to rely on quantitative indicators of salt removal, averaged over sufficiently large areas and sufficiently long time intervals. We define separate areas as the entire basin of the Aral Sea (the roughest approximation), each of three regions separately or (if this is necessary and corresponding quantitative indicators are available), a subregion within a region. A separate subregion may be simulated as a point, linear, or 2D source with a given intensity. As a time unit, a year (a month, or a day) can be taken.

Below we consider the simulation data on salt removal from point, linear, and 2D sources for a one-layer model of the atmospheric boundary layer.

3. ONE-LAYER PROBLEM, ANALYTIC SOLUTIONS

3.1 Simulation of the emission region as a point source

Convective diffusion Eq.(2) can be written as

$$u\frac{\partial c}{\partial x} = \frac{\partial}{\partial z}\left(k_z\frac{\partial c}{\partial z} - wc\right) + \frac{\partial}{\partial y}\left(k_y\frac{\partial c}{\partial y}\right) \tag{9}$$

for the space region

$\{x, y, z: 0 < x < \infty, -\infty < y < \infty, 0 < z < \infty\}$; k_y is defined by Eq.(7).

Following by Berlyand (1975), we search for the solution to this equation as

$$c(x, y, z) = c_1(x, z)c_2(x, y) \tag{10}$$

Let us introduce the function

$$\widetilde{C}_i = \begin{cases} C_i & ,x > 0, z > 0, -\infty < y < \infty, \\ 0 & ,x < 0, z > 0, -\infty < y < \infty. \end{cases} \tag{11}$$

Then Eq.(9) splits into two,

$$u\frac{\partial \widetilde{C}_1}{\partial x} = \frac{\partial}{\partial z}\left[k_z\frac{\partial \widetilde{C}_1}{\partial z} - w\widetilde{C}_1\right.$$

$$+u[\widetilde{C_1}(x,z)]_{x=0}\delta(x), \tag{12}$$

$$u\frac{\partial \widetilde{C_2}}{\partial x}=\frac{\partial}{\partial y}[k_y\frac{\partial \widetilde{C_2}}{\partial y}]+u[\widetilde{C_2}(x,y)]_{x=0}\delta(x),\ , \tag{13}$$

where $[\widetilde{C_i}]=C_i\mid_{x=\pm 0}-C_i\mid_{x=-0}$ and (x) is the Dirac function.

Let us accept that the wind velocity u and the turbulent exchange coefficients are defined by Eq.(5) and Eq.(7).

If the logarithmic velocity distribution is approximated by the power distribution

$$u=u_1\frac{\log(z/z_0)}{\log(z_1/z_0)}\cong u_1\left(\frac{z}{z}\right)^{n_0} \tag{14}$$

where the exponent n_0 is selected so that the exact and approximate velocities coincide at $z=h$, that is, at the upper boundary of the surface layer, Eq.(13) takes on the form

$$u\frac{\partial \widetilde{C_2}}{\partial x}=k_0\frac{\partial^2 \widetilde{C_2}}{\partial y}+[\widetilde{C_2}(x,y)]_{x=0}\delta(x) \tag{15}$$

Let us set $[\widetilde{C_2}]_{x=0}=\delta(y)$ and, as a solution to Eq.(15) in the form of heat conduction, we select the known function of the source,

$$c_2(x,y)=\frac{1}{2\sqrt{\pi k_0 x}}\exp\left(-\frac{y^2}{4k_0x}\right) \tag{16}$$

(Hereafter we omit the overbar above c_i.)

Eq.(12) can be written as

$$\overline{u}\frac{\partial C_1}{\partial x}=\frac{\partial}{\partial z}(\overline{k_z}\frac{\partial C_1}{\partial z})+[C_1(x,z)]_{x=0}\delta(x) \tag{17}$$

where

$$\overline{u}=u\exp(-w\int_{z_1}^{z}\frac{dz}{k_z}),$$

$$\overline{k_z}=k_z\exp(-w\int_{z_1}^{z}\frac{dz}{k_z}) \tag{18}$$

We search for the function of point source influence; therefore, the boundary conditions are given by

$$\overline{u}[C_1(x,z)]_{x=0}=M\delta(x), \tag{19}$$

where M is the source strength. Furthermore, we require decreasing the impurity concentration at an infinite distance from the source,

$$c(x,y,z)\to 0,\ \sqrt{x^2+y^2+z^2}\to\infty. \tag{20}$$

The functions $\overline{k_z}$ and $\overline{u}$ are approximated by the power dependences according to Eq.(5) and Eq.(18),

$$\overline{k_z}=k_1(\frac{z}{z_1})^{1-w},\overline{u}=u_1(\frac{z}{z_1})^{n_0-w},$$

$$\overline{w}=\frac{wz_1}{k_1} \tag{21}$$

A solution to Eq.(17) with boundary conditions Eq.(19) and Eq.(20) can be obtained using the Laplace transformation over the variable x,

$$c_1(x,y,z)=A_0\frac{M}{x^{\mu+1}}\exp\left(-\frac{w_1^{\,2}z^{1+n_0}}{x}\right) \tag{22}$$

where

$$A_0=\frac{(u_1/k_1)^{\mu}z_1^{\,1-\overline{w}+(1-n_0)\mu}}{k_1(1+n_0-\overline{w})^{2\mu+1}\Gamma(\mu+1)},$$

$$w_1^{\,2}=\frac{z_1^{\,1-n_0}}{(1+n_0)^2k_1}\frac{u_1}{k_1},\ \mu=-\frac{\overline{w}}{n_0+1} \tag{23}$$

Thus, according to Eq(10), Eq(16), and Eq.(22), the influence function c_u of the source with the power M, active at the point $(0,0,0)$, is given by

$$c_u(x,y,z)=\frac{A_0M}{x^{\mu+1}}\frac{1}{2\sqrt{\pi k_0x}}\exp\left(-\frac{w_1^{\,2}z^{1+n_0}}{x}-\frac{y^2}{4k_0x}\right) \tag{24}$$

As follows from Eq.(24), the concentration exponentially decreases with altitude as receding in the lateral wind direction also (with the exponents z^{1+n_0} and y^2 respectively). The concentration decrease along the wind direction is of the order of $x^{\mu+3/2}$. An interesting feature of this distribution is a concentration maximum at the fixed altitude $z=z_m$. At the distance $y=y_m$ from the x axis, the maximum is reached at the point

$$x_m=\frac{w_1^{\,2}z_m^{\,1+n_0}+y_m^{\,2}/4k_0}{\mu+3/2} \tag{25}$$

The highest concentration is reached at $y_m=0$; hence most of the impurity is concentrated in a narrow plume region oriented along the x axis.

3.2 Two-dimensional source

Let salts be removed from the area $0\le x\le x_0$, $|y|<l$. The strength of the source continuously distributed over this area is $q_1(x)\ q_2(y)$ ($q_2\equiv 1$); hence the salt mass removed from the entire area is given by

$$M=\int_{-l}^{l}\int_{0}^{x_0} q_1(x)\ q_2(y)\,dxdy=2l\int_{0}^{x_0} q_1(x)\,dx$$

The influence function of this 2D source is given by

$$c_{ss}(x,y,z)=\frac{A_0}{2}\int_0^{x^*}\frac{q_1(\xi)}{(x-\xi)^{\mu+1}}\exp\left(-\frac{w_1^{\,2}z^{1+n_0}}{x-\xi}\right)\left[\mathrm{erf}\ \frac{y+1}{2\sqrt{k_0(x-\xi)}}-\mathrm{erf}\ \frac{y-1}{2\sqrt{k_0(x-\xi)}}\right]d\xi \quad (26)$$

where $x^*=x$, $x<x_0$; $x^*=0$, $x>x_0$.

Let us consider the case $q_1(x)=q_0=M/2lx_0=const.$ At $0<x<x_0$, we have $\partial c_{ss}/\partial x=(q_0/M)\,c_{ls}(x,y_m,z_m)>0$; hence there are no maxima at $0<x<x_0$.

If $x>x_0$, at the extreme points, the equation

$$\left.\frac{\partial c_{ss}}{\partial x}\right|_{\substack{y=y_m\\z=z_m}}=\frac{q_0}{M}[\,c_{ls}(x,y_m,z_m)-c_{ls}(x-x_0,y_m,z_m)]=0 \quad (27)$$

is valid. It is convenient to determine the square root of this equation using the graphic method shown in Fig.1.

As the figures show, the maximum point $x=x_{ss}$ of the 2D source is in both cases between the maxima of the linear sources positioned in the sections $x=0$ and $x=x_0$, respectively.

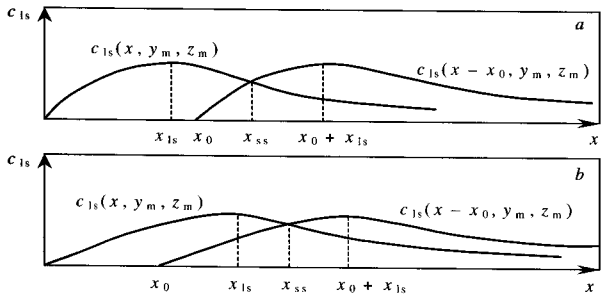

Fig. 1 Graphic representation of the solution to the problem of the c_{ss} maximum of the concentration function (see Eq.(26)), x_{ss} is this maximum; $0\le x\le x_0$ (a) and $x>x_0$ (b)

4. APPLICATION OF RESULTS

As is known, salt and saliferous sand are removed immediately from sea water, drained sea bottom areas, and saline lands. By Tolkachyova (2000), their total area S reached 72000 km^2 in 1990, and the total yearly removal of salts, M, from this area was 120 million tons. The emission area is oblong extended from northeast (NE) to southwest (SW). Taking this into account, as well as a long-term forecast of salt precipitation onto territories far from the Sea, the emission area can be simulated by a rectangle prolate from NE to SW. The coordinate system is selected taking into account the wind direction, the positive x axis direction should coincide with the wind direction, the positive y axis direction makes 90° with the x axis counter-clockwise. The z axis is directed vertically upwards.

The dominant wind (dust and salt removal) directions are north and northeast by Tolkachyova (2000) and Rafikov (1982). Taking this into account, the rectangle under consideration will be $\{0<x<L, |y|<l\}$, where L and $2l$ are its length and width, respectively.

Let the salt removal intensity Q depend only on x, that is, $M=2l\int_0^L Q(x)dx$.

Then the concentration distribution of salts carried with the wind along the x axis from such a 2D source is defined by Eq.(26).

The dust and salt removal was calculated for particles of various size with the following parameters: $k_1=0.2\ m^2\cdot s^{-1}$, $k_0=0.5m$, $n_0=0.15$, $z_1=1m$, $L=450km$, $l=79.5km$, $Q=1/219kg\cdot m^{-2}\cdot day^{-1}$.

Let the removal intensity Q be constant and identical for the entire emission area. Then $Q=M/ST$, where $T=1$ or 365 if a time unit is 1 yr or 1day, respectively.

The results calculated for the section $y=0$ are listed in Table 2.

Table 2 lists the amounts of particle precipitation (ton · hectare yr^{-1}) depending on the particle diameter d the distance $x-L$. The calculated results are valid in the entire band $|y|<l$ except for the narrow boundary strip $l-3\sqrt{k_0x}<|y|<1$, where precipitation sharply decreases. At the outer boundary $|y|<l$ of this strip, the precipitation mass is almost two times less than at its inner boundary $|y|=l-3\sqrt{k_0x}$. The boundary strip widens as receding from the source. At a distance of 500 km from the source, its width is 1.5 km at $k_0=0.5m$.

Table 2 The amount of particle precipitation (ton · hectare^{-1} · yr^{-1}) versus the particle diameter d and the distance $x-L$ calculated for the section $y=0$

w_0, $m \cdot s^{-1}$	d, μm	$x-L$, km							
		25	50	100	200	300	400	500	1000
0.30	96.08	0.0012	0.0005	0.0002	0	0	0	0	0
0.20	78.44	0.0260	0.0130	0.0065	0.0029	0.0018	0.0012	0.0008	0.0003
0.10	55.49	0.4800	0.3130	0.1910	0.1080	0.0740	0.0560	0.0440	0.0199
0.05	39.22	1.7180	1.2310	0.8330	0.5230	0.3830	0.3010	0.2470	0.1260
0.01	17.55	1.4830	1.1410	0.8300	0.5630	0.4330	0.3530	0.2980	0.1680
0.001	5.55	0.0250	0.1600	0.1180	0.0820	0.0630	0.0520	0.0440	0.0260
$1.3 \cdot 10^{-4}$	2.00	0.0280	0.0216	0.0159	0.0110	0.0086	0.0071	0.0060	0.0035
$3.25 \cdot 10^{-5}$	1.00	0.0069	0.0054	0.0040	0.0027	0.0022	0.0018	0.0015	0.0008

Fig. 2 shows the precipitation rates q_0 versus the distance to the source for its various area $S=2lL$ (L is the variable length).

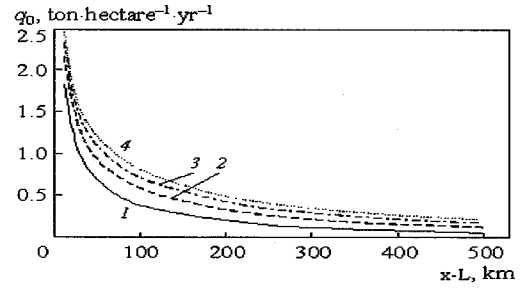

Fig. 2 Dependence of the precipitation rate q_0 on the distance to the source for its various areas $S=2lL$; $L=10^5$ (curve 1), $2 \cdot 10^5$(2), $3 \cdot 10^5$(3) and $4 \cdot 10^5$ km (4)

As L increases, at first precipitation appreciably increases (up to 25% at a distance of 25km), then the increase rate drops. At $L=400$ km, most precipitation falls onto the sea water area.

5. CONCLUSIONS

According to the calculated results, the transport and precipitation of solid particles in this strip essentially depend, apart from the hydrodynamic parameters, on their size. For example, at distances of 100-1000 km from the emission area, large particles about 40 μm in diameter are subject to the strongest precipitation. Most larger particles precipitate at distances from several hundred meters to several kilometers. Coarsely dispersed particles 5 μm in diameter, medium dispersed, and the more so finely dispersed particles precipitate at the above-mentioned distances in much smaller amounts. Their major portion is carried over distances longer than 1000 km.

As follows from the above considerations, the emission area for the wind transport of salt and saliferous sand from the Aral Sea basin can be simulated as a 2D source with a constant intensity in the long-term forecast calculations. In this case, apart from wind frequency, various size fractions in the main body of yearly removal should be taken into account.

ACKNOWLEDGMENT

This study was supported by research funds from Chosun university, 2004.

REFERENCES

Batchelor, G.K. (1953). The Theory of Homogeneous Turbulence, Cambridge University Press, Cambridge.

Begmatov, A., Makhmudov, E.Zh. and Muminova, M.N. (2002). To the Problem of Non-stationary Motion of Impurities, Problems of Mechanics, No 4, pp 25-30.

Berlyand, M.E. (1975). Modern Problems of Atmospheric Diffusion and Atmospheric Pollution, Gidrometeoizdat, Leningrad.

Berlyand, M.E. (1985). Forecast and Monitoring of Atmospheric Pollution, Gidrometeoizdat, Leningrad.

Kolmogorov, A.N. (1991). The Local Structure of Turbulence in an Incompressible Viscous Fluid for very large Reynolds numbers, Proc. Roy. Soc. London Ser. A, Vol 434, pp 9-13.

Loitsyansky, L.G. (1970). Mechanics of Liquid and Gas, Nauka, Moscow.

Lysakand, A.V. and Ryaboshenko, A.G. (1987). Calculation of Atmospheric Impurity Precipitation from a 2-D Source, Gidrometeoizdat, Moscow.

Marchuk, G.I. (1982). Mathematical Modeling in the Environmental Problems, Nauka, Moscow.

McComb, W.D. (1992). The Physics of Fluid Turbulence, Oxford University Press, Oxford.

Monin, A.S. and Yaglom, A.M. (1979). Statistical Fluid Mechanics: Mechanics of Turbulence, MIT press, Cambridge, Massachusetts.

Obukhov, A.M. (1962). Some Specific Features of Atmospheric Turbulence, J. of Fluid Mech., Vol 13, pp 77-81.

Rafikov, A.A. (1982). Environment of the Drained Southern Coast of the Aral Sea, Fan, Tashkent.

Richardson, L. (1922). Weather Prediction by Numeric Process, Cambridge University Press, Cambridge.

Tolkachyova, G.A. (2000). Scientific and Methodical Fundamentals of Monitoring of Atmospheric Precipitations in the Central Asian Region, SANIGMI, Tashkent.

2005년 2월 7일 원고 접수
2005년 5월 30일 수정본 채택